

# Illumination Invariant Color Texture Analysis Based on Sum- and Difference-Histograms

Christian Münzenmayer<sup>1</sup>, Sylvia Wilharm<sup>2</sup>,  
Joachim Hornegger<sup>2</sup>, and Thomas Wittenberg<sup>1</sup>

<sup>1</sup> Fraunhofer Institut für Integrierte Schaltungen,  
Am Wolfsmantel 33, D-91058 Erlangen

{mzn, wbg}@iis.fraunhofer.de

<sup>2</sup> Lehrstuhl für Mustererkennung, Universität Erlangen-Nürnberg,  
Martensstr. 3, D-91058 Erlangen

Joachim.Hornegger@informatik.uni-erlangen.de

**Abstract.** Color texture algorithms have been under investigation for quite a few years now. However, the results of these algorithms are still under considerable influence of the illumination conditions under which the images were captured. It is strongly desirable to reduce the influence of illumination as much as possible to obtain stable and satisfying classification results even under difficult imaging conditions, as they can occur e.g. in medical applications like endoscopy. In this paper we present the analysis of a well-known texture analysis algorithm, namely the sum- and difference-histogram features, with respect to illumination changes. Based on this analysis, we propose a novel set of features factoring out the illumination influence from the majority of the original features. We conclude our paper with a quantitative, experimental evaluation on artificial and real image samples.

## 1 Introduction

For many years the automatic analysis and classification of structured surfaces in color images has been an active field of research in the image processing and pattern recognition community. Currently, there exists a wide range of texture and color texture methods, and an ongoing development of new methods, even for pure gray level image material. Texture features may be divided into the categories *spectral*, *statistical* and *model-based* features [14]. The most common spectral features are based on spectral transforms whereas many statistical methods use so-called co-occurrence matrices or *sum- and difference-histograms* [16,10]. Color texture analysis has been of increasing interest in the last few years with important works of Tan and Kittler [15] proposing a parallel approach to 'color texture', i.e. color and texture features are extracted separately. Alternatively, integrated color and texture extraction techniques have been developed [7,2,9,12]. Basically, all of these expand concepts of gray level analysis to the color domain, whereas some of them emphasize on different color spaces as well [13,3]. Most of these techniques were developed and evaluated on more or less artificial sample images which were taken under laboratory conditions. Robustness

against changing color temperature of light sources or inhomogeneous illumination conditions as required by practical applications is still not very common, with only few new approaches recently known [4,6,21,20,11]. The present work addresses exactly this problem assuming a global color temperature change of the light source.

In the next section we will introduce the linear model of illumination change. Section 3 summarizes the definition of the *intra-* and *inter-plane* sum- and difference-histograms published by Unser [16] and its color extension in [10]. These well known features will be analysed and a modification will be proposed in Section 4 with an experimental evaluation following in Section 5. We will conclude our contribution by a short discussion in Section 6.

## 2 Linear Model of Illumination Change

For image formation we assume a linear model which is widely known as state of the art [19,8,18]. It models the linear sensor response  $\rho^{(k)}$  for the  $k$ 'th spectral band as the result of the integration of spectral radiance of the light source  $E(\lambda)$  with wavelength  $\lambda$ , the spectral reflectivity of the surface  $s(\lambda)$  and the sensor's sensitivities  $R^{(k)}(\lambda)$ :

$$\rho^{(k)} = \int_{\lambda} R^{(k)}(\lambda)E(\lambda)s(\lambda)d\lambda. \quad (1)$$

For simplicity of our analysis we omit any references to the surface, illumination and viewing geometry, commonly expressed by the emitting light source vector and the surface normal vector, and to camera parameters like integration time or gamma correction non-linearities. In his fundamental work [19], Wandell uses low-dimensional *linear models* for the representation of spectral reflectance and illuminant functions. Using  $D_E$  and  $D_s$  basis functions  $E_i(\lambda)$  and  $s_j(\lambda)$ , respectively, the illumination  $E(\lambda)$  and surface reflectivity  $s(\lambda)$  can be formulated as:

$$E(\lambda) = \sum_{i=0}^{D_E-1} \epsilon_i E_i(\lambda), \quad s(\lambda) = \sum_{j=0}^{D_s-1} \sigma_j s_j(\lambda). \quad (2)$$

There exist many possibilities to select basis functions, e.g. *Fourier* expansion, or a basis derived from a *principal components analysis* of a representative spectral reflectance set. Now, if the illuminant is known by its coefficients  $\epsilon_i$ , the *linear image formation model* (1) can be reduced to

$$\rho = \mathbf{A}_E \boldsymbol{\sigma} \quad (3)$$

where  $\boldsymbol{\sigma}$  is a column vector of surface basis function coefficients  $\sigma_j$  and  $\mathbf{A}_E$  is the lighting matrix where the  $kj$ th entry is

$$A_{E,kj} = \sum_{i=0}^{D_E-1} \epsilon_i \int_{\lambda} R^{(k)}(\lambda)E_i(\lambda)s_j(\lambda)d\lambda. \quad (4)$$

Note that  $\mathbf{A}_E$  depends only on the light source ( $\epsilon_i$  and  $E_i(\lambda)$ ), the surface basis functions  $s_j(\lambda)$  and the sensor characteristics  $R^{(k)}(\lambda)$  but not on the actual surface reflectance coefficients  $\sigma_j$ . Thus, in case of an illumination change, there will be alterations in  $\mathbf{A}_E$  which affect each surface point equivalently. Following the work of Barnard [1], we assume a 3-dimensional surface reflection model ( $D_s = 3$ ). Note, that there is no restriction on the dimensionality of the illumination spectrum ( $D_E$ ). Thus, with  $K = 3$  color sensors, we obtain a  $3 \times 3$  lighting matrix  $\mathbf{A}_E$ . Now, let  $\rho^{E1} = \mathbf{A}_E^{E1} \sigma$  be the sensor response under illumination E1 and  $\rho^{E2} = \mathbf{A}_E^{E2} \sigma$  the response under E2. Substituting the common term  $\sigma$ , it can be shown easily that

$$\rho^{E2} = \underbrace{\mathbf{A}_E^{E2} (\mathbf{A}_E^{E1})^{-1}}_{\mathbf{M}} \rho^{E1}, \quad (5)$$

i.e. the illumination change induces a linear transform of the sensor responses by a  $3 \times 3$  matrix  $\mathbf{M}$ . Assuming narrow-band sensors, a diagonal transformation  $\mathbf{D}$  can be used as an approximation which is known in color constancy literature as the von Kries coefficient rule [1].

### 3 Sum- and Difference-Histograms in Color Space

In this section we introduce the sum- and difference histogram features as proposed by Unser [16]. They are based on the so-called co-occurrence features introduced by Haralick [5] which are based on an estimate of the joint probability function of pixels in certain spatial relationships. Sum- and difference-histograms provide an efficient approximation for the joint probability by counting the frequencies of sums respectively differences of pixel pairs

$$\pi_{r\theta} = [(x_1, y_1), (x_2 = x_1 + r \cos \theta, y_2 = y_1 + r \sin \theta)] \quad (6)$$

with the radial distance  $r$  and the angular displacement  $\theta$ . With  $G$  being the maximum intensity level these histograms are defined as:

$$h_S(i) = |\{\pi_{r\theta} | I(x_1, y_1) + I(x_2, y_2) = i\}|, \quad (7)$$

$$h_D(j) = |\{\pi_{r\theta} | I(x_1, y_1) - I(x_2, y_2) = j\}|, \quad (8)$$

with  $i = 0, \dots, 2(G - 1)$  and  $j = -G + 1, \dots, G - 1$ . In general, it is sufficient to use  $\theta \in \{0, \pi/4, \pi/2, 3\pi/4\}$  and a small radius  $r$ , and calculate features on each of the histograms separately. The approximative probabilities are derived by normalization with the total number of pixels  $N$  in the considered image region of interest:

$$p_S(i) = \frac{h_S(i)}{N}, \quad p_D(j) = \frac{h_D(j)}{N}. \quad (9)$$

Integrated color texture extraction by *intra-* and *inter-plane* sum- and difference-histograms

$$h_{S,D}^{(pq)}(i) = \left| \left\{ \pi_{r\theta} | I^{(p)}(x_1, y_1) \pm I^{(q)}(x_2, y_2) = i \right\} \right| \quad (10)$$

was presented in [10] and will be reviewed shortly here. Here, joint probabilities over different color channels  $p, q \in \{R, G, B\}$  are approximated and evaluated by the same features as in the gray level case. In the following *intra-plane* features are computed from pixel pairs within each plane  $p = q$  and *inter-plane* features from distinct planes  $p \neq q$ . All features for different directions  $\Theta$  and different *intra-* or *inter-plane* combinations are concatenated to the final feature vector which is used for classification.

## 4 Deriving Illumination Invariant Features

The next section is dedicated to the analysis of the sum- and difference-histograms and derived features in context of a *multiplicative* or *diagonal* illumination change. A multiplicative illumination change has influence only on the brightness of an image pixel and can be modeled by a multiplicative factor  $k$ . In consequence the sum- and difference-histograms change by:

$$\begin{aligned} \hat{h}_{S,D}^{(pq)}(i) &= \left| \left\{ \pi_{r\Theta} | k \cdot I^{(p)}(x_1, y_1) \pm k \cdot I^{(q)}(x_2, y_2) = i \right\} \right| \\ &= \left| \left\{ \pi_{r\Theta} | I^{(p)}(x_1, y_1) \pm I^{(q)}(x_2, y_2) = i/k \right\} \right| = h_{S,D}^{(pq)}(i/k). \end{aligned} \quad (11)$$

This is true for *intra-plane* ( $p = q$ ) and *inter-plane* ( $p \neq q$ ) histograms, not counting quantization errors. For the *diagonal model*, the illumination change is equivalent to an independent scaling of each color channel by a separate factor  $k_p$ . *Intra-plane* histograms will therefore change similarly. Thus, in the following considerations we will restrict ourselves only to the *intra-plane* model with *multiplicative* and *diagonal* illumination change.

Unser [16] proposed a set of 15 features based on the normalized sum- and difference distributions  $p_S(i)$  and  $p_D(j)$  (see Table 1) which will be analysed with regard to the influence of illumination changes. Therefore, we try to express the value of a feature under illumination change  $\hat{c}$  as a function of the feature  $c$  under unchanged illumination. As an example, we derive the following change for the feature *sum mean*  $c_0$ :

$$\hat{c}_0 = \hat{\mu}_s = \sum_i \hat{p}_s(i) \cdot i = \sum_i p_s(i/k) \cdot i = \sum_{i'} p_s(i') \cdot ki' = k \cdot c_0 \quad (12)$$

As can be seen, the feature  $c_0$  is scaled by the factor of the multiplicative illumination change. Similarly, the feature *sum variance*  $c_1$  can be considered and reformulated by variable substitution:

$$\hat{c}_1 = \sum_i (i - \hat{\mu}_s)^2 \hat{p}_s(i) = \sum_i (i - k\mu_s)^2 p_s(i/k) = \sum_{i'} (ki' - k\mu_s)^2 p_s(i') = k^2 c_1 \quad (13)$$

In this case the feature  $c_1$  is scaled by the square of the illumination change. We conducted this analysis on all 15 features with the summary of results in Table 1. In total 6 of 15 features, namely sum energy  $c_2$ , sum entropy  $c_3$ , diff energy  $c_6$

**Table 1.** Scalar texture features derived from sum- and difference-histograms with the original features by Unser [16] and the same features under illumination change with multiplicative and intra-plane model and modified features invariant against illumination changes

Features	Original Definition	Illumination Change $I^{(p)} = k_p \cdot I^{(p)}$	New Definition
sum mean	$c_0 = \mu_s = \sum_i i p_s(i)$	$\hat{c}_0 = k \cdot c_0$	-
sum variance	$c_1 = \sum_i (i - \mu_s)^2 p_s(i)$	$\hat{c}_1 = k^2 \cdot c_1$	$\hat{c}'_1 = \frac{\hat{c}_1}{\mu_s^2} = \frac{c_1}{\mu_s^2}$
sum energy	$c_2 = \sum_i p_s^2(i)$	$\hat{c}_2 = c_2$	$\hat{c}'_2 = \hat{c}_2 = c_2$
sum entropy	$c_3 = -\sum_i p_s(i) \log p_s(i)$	$\hat{c}_3 = c_3$	$\hat{c}'_3 = \hat{c}_3 = c_3$
diff mean	$c_4 = \mu_d = \sum_j j p_d(j)$	$\hat{c}_4 = k \cdot c_4$	$\hat{c}'_4 = \frac{\hat{c}_4}{\mu_s} = \frac{c_4}{\mu_s}$
diff variance	$c_5 = \sum_j (j - \mu_d)^2 p_d(j)$	$\hat{c}_5 = k^2 \cdot c_5$	$\hat{c}'_5 = \frac{\hat{c}_5}{\mu_s^2} = \frac{c_5}{\mu_s^2}$
diff energy	$c_6 = \sum_j p_d^2(j)$	$\hat{c}_6 = c_6$	$\hat{c}'_6 = \hat{c}_6 = c_6$
diff entropy	$c_7 = -\sum_j p_d(j) \log p_d(j)$	$\hat{c}_7 = c_7$	$\hat{c}'_7 = \hat{c}_7 = c_7$
cluster shade	$c_8 = \sum_i (i - \mu_s)^3 p_s(i)$	$\hat{c}_8 = k^3 \cdot c_8$	$\hat{c}'_8 = \frac{\hat{c}_8}{\mu_s^3} = \frac{c_8}{\mu_s^3}$
cluster prominence	$c_9 = \sum_i (i - \mu_s)^4 p_s(i)$	$\hat{c}_9 = k^4 \cdot c_9$	$\hat{c}'_9 = \frac{\hat{c}_9}{\mu_s^4} = \frac{c_9}{\mu_s^4}$
contrast	$c_{10} = \sum_j j^2 p_d(j)$	$\hat{c}_{10} = k^2 \cdot c_{10}$	$\hat{c}'_{10} = \frac{\hat{c}_{10}}{\mu_s^2} = \frac{c_{10}}{\mu_s^2}$
homogeneity	$c_{11} = \sum_j \frac{1}{1+j^2} p_d(j)$	$\hat{c}_{11} = \sum_{j'} \frac{1}{1+(kj')^2} p_d(j')$	-
correlation	$c_{12} = c_1 - c_{10}$	$\hat{c}_{12} = k^2 \cdot c_{12}$	$\hat{c}'_{12} = \frac{\hat{c}_{12}}{\mu_s^2} = \frac{c_{12}}{\mu_s^2}$
angular 2nd moment	$c_{13} = c_2 \cdot c_6$	$\hat{c}_{13} = c_{13}$	$\hat{c}'_{13} = \hat{c}_{13} = c_{13}$
entropy	$c_{14} = c_3 + c_7$	$\hat{c}_{14} = c_{14}$	$\hat{c}'_{14} = \hat{c}_{14} = c_{14}$

and diff entropy  $c_7$  as well as the total entropy  $c_{14}$  and the angular second moment  $c_{13}$  are invariant under this model of illumination change. That means, that more than half of all features are affected by diagonal illumination changes, thus degrading classification performance. From Table 1 it is also obvious, that all other features except *homogeneity*  $c_{11}$  contain a power of  $k$  as a multiplicative factor. Therefore, we propose to normalize these features except  $c_0$  by a power of the sum mean  $c_0 = \mu_s$ , thus canceling out the factor  $k$ . Normalizing e.g. the *sum variance*  $c_1$  yields

$$\hat{c}'_1 = \frac{\hat{c}_1}{\hat{c}_0^2} = \frac{k^2 c_1}{k^2 c_0^2} = \frac{c_1}{c_0^2}. \quad (14)$$

All modifications are summarized in Table 1 representing a new set of illumination invariant features  $c'$ .

## 5 Experiments and Results

To validate our newly defined texture features we used two different color image sets. The first one is taken from the *VisTex (Vision Texture)* database [17] published by the *MIT*. We selected 32 images showing different color textures (also used in [9,10]). We selected 10 disjoint  $64 \times 64$  pixel regions of interest (ROI) in

each image for training of a *k nearest neighbor* classifier and another set of 10 regions per image for validation of the classification performance. To simulate illumination changes complying with the diagonal model, we calculated diagonal transform matrices based on the  $\mathbf{RGB}_{\text{CIE}}$ -system by linear least squares regression. As there is no illumination related information available about the origin of the VisTex images, we assumed transformations from *CIE* daylight illuminant D55 with 5500 K *CCT* (*correlated color temperature*) to six different color temperatures in the range of 4000 to 7000 K. This leads to a color shift from a reddish (4000 K) to a bluish (7000 K) tint. To avoid clipping artefacts by coefficients  $> 1$ , the gray level dynamic of the original images was compressed by the factor 0.8.

The second data set we used, originates from a medical application of color texture analysis for the classification of different types of mucous tissue inside the esophagus. All images were acquired by a high-resolution magnification endoscope<sup>3</sup> after application of acid solution to enhance mucous structures. For each tissue class, irregularly bounded ROI's were classified by clinical experts with histologic confirmation by conventional biopsy. The whole data set includes 390 images with a total of 482 ROI's.

All texture features were individually normalized to  $\mu = 0$  and  $\sigma = 1$  on the training data set to ensure equal weighting in the calculation of the classifier's distance function. Fig. 1(a) shows the classification accuracy of the original and the illumination invariant features with and without the variant feature  $c_{11}$  for different diagonal illumination changes. Note that at 5500 K no illumination change takes place as we have chosen to use this point as the reference illumination. For the endoscopic data set Fig. 1(b) summarizes the classification accuracy in a leaving-one-out setting. We gathered results for the original image resolution of  $768 \times 576$  pixels and 3 further reduction steps of a Gaussian multiresolution pyramid which proved advantageous in previous experiments and is advantageous to reduce computation time. In every case the illumination invariant feature set is superior to the original definition. However, the variant feature  $c_{11}$  (homogeneity) seems to have a strong contribution on the final result so that it should not be excluded despite its obvious dependency on the illumination.

## 6 Discussion

In this work we presented the analysis of the sum- and difference histogram color texture features [10,16] with respect to changes in the spectral characteristics of the illumination. We modeled illumination changes by a diagonal transformation matrix based on a linear image formation model and have shown how the sum- and difference-histograms change with the coefficients of this matrix. Based on this analysis, we have presented novel definitions for features which are invariant to the considered illumination change.

Experiments on artificial and real images have shown that improvements in classification accuracy can be obtained by such a normalization. However, the

<sup>3</sup> Olympus GIF Q160Z.

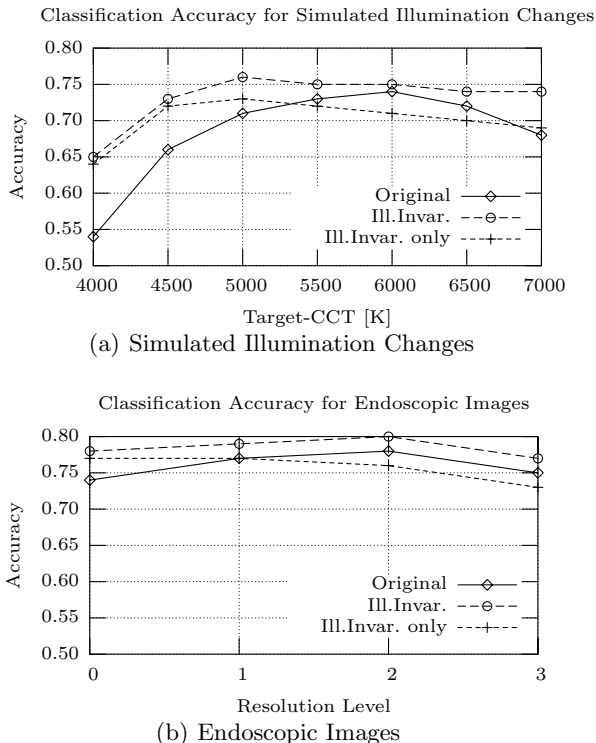


**Fig. 1.** Classification accuracy for sum- and difference-histogram features shown for the *original* features of Unser, our illumination invariant features including the variant feature  $c_{11}$  (*Ill.Invar.*) and without  $c_{11}$  (*Ill.Invar. only*). (a) Simulated diagonal illumination changes on VisTex images assuming  $\mathbf{RGB}_{CIE}$ -system with transformations from 5500 K to a range of 4000 to 7000 K. (b) Classification of real endoscopic images of the esophagus for different resolutions in a multiresolution Gaussian pyramid.

amount of improvement naturally depends on the degree of change in the illumination, e.g. with 4000 K an improvement of 11% has been reached compared with only 2% in the reference case (5500 K). For the endoscopic data set a maximum improvement of 4% for the original resolution and 2% for the reduced resolutions is a sign for the stability of the light source with respect to aging. Of course stronger improvements are expected for applications under natural light, e.g. in outdoor scenarios.

## References

1. K. Barnard. Modeling scene illumination colour for computer vision and image reproduction: A survey of computational approaches. Technical report, Simon Fraser University, Vancouver, B.C., Canada, 1998.
2. G. V. de Wouwer, P. Scheunders, S. Livens, and D. V. Dyck. Wavelet correlation signatures for color texture characterization. *Pat. Rec.*, 32(3):443–451, 1999.

3. A. Drimbarean and P. Whelan. Experiments in colour texture analysis. *Pat. Rec. Letters*, 22:1161–1167, 2001.
4. G. Finlayson, S. Chatterjee, and B. Funt. Color angular indexing. In *ECCV (2)*, pages 16–27, 1996.
5. R. Haralick, K. Shanmugam, and I. Dinstein. Textural features for image classification. *IEEE Trans. Syst. Man Cyb.*, SMC-3(6):610–621, November 1973.
6. G. Healey and D. Slater. Computing illumination-invariant descriptors of spatially filtered color image regions. *IEEE Trans. Image Process.*, 6(7):1002–1013, July 1997.
7. A. Jain and G. Healey. A Multiscale Representation Including Opponent Color Features for Texture Recognition. *IEEE Trans. Image Process.*, 7(1):124–128, January 1998.
8. J.H., B. Funt, and M. Drew. Separating a color signal into illumination and surface reflectance components: Theory and applications. *IEEE Trans. Pattern Anal. Mach. Intell.*, 12(10):966–977, October 1990.
9. R. Lakmann. *Statistische Modellierung von Farbtexturen*. PhD thesis, Universität Koblenz-Landau, Koblenz, 1998.
10. C. Münzenmayer, H. Volk, C. Küblbeck, K. Spinnler, and T. Wittenberg. Multispectral Texture Analysis using Interplane Sum- and Difference-Histograms. In L. V. Gool, editor, *Pattern Recognition - Proceedings of the 24th DAGM Symposium Zurich, Switzerland, September 2002*, pages 25–31, Berlin, 2002. Springer.
11. T. Ojala, M. Pietikäinen, and T. Mäenpää. Multiresolution gray-scale and rotation invariant texture classification with local binary patterns. *IEEE Trans. Pattern Anal. Mach. Intell.*, 24(7):971–987, 2002.
12. C. Palm. *Integrative Auswertung von Farbe und Textur*. PhD thesis, RWTH Aachen, Osnabrück, 2003.
13. G. Paschos. Perceptually Uniform Color Spaces for Color Texture Analysis: An Empirical Evaluation. *IEEE Trans. Image Process.*, 10(6):932–937, June 2001.
14. T. Randen and J. H. Husoy. Filtering for texture classification: A comparative study. *IEEE Trans. Pattern Anal. Mach. Intell.*, 21(4):291–310, April 1999.
15. T. Tan and J. Kittler. Colour texture analysis using colour histogram. In *IEE Proc.-Vis. Image Signal Process.*, volume 141, pages 260–26, December 1994.
16. M. Unser. Sum and difference histograms for texture analysis. *IEEE Transactions on Pattern Analysis and Machine Intelligence*, 8(1):118–125, 1986.
17. M. M. L. Vision and M. group. Vistex vision texture database, <http://www-white.media.mit.edu/vismod/imagery/visiontexture>, 1995.
18. P. Vora, J. Farrell, J. Tietz, and D. Brainard. Linear models for digital cameras. In *Proc. of the 1997 IS&T 50th Annual Conference*, pages 377–382, Cambridge, MA, 1997.
19. B. Wandell. The synthesis and analysis of color images. *IEEE Trans. Pattern Anal. Mach. Intell.*, 9(1):2–13, January 1987.
20. J. F. C. Wanderley and M. H. Fisher. Multiscale color invariants based on the human visual system. *IEEE Trans. Image Process.*, 10(11):1630–1638, November 2001.
21. L. Wang and G. Healey. Using zernike moments for the illumination and geometry invariant classification of multispectral texture. *IEEE Trans. Image Process.*, 7(2):196–203, February 1998.